González, V., Monje, C.A., Moreno, L., Balaguer, C. (2017). UAVs mission planning with flight level constraint using Fast Marching Square Method, *Robotics and Autonomous Systems*, v. 94, pp.: 162-171.

DOI: https://doi.org/10.1016/j.robot.2017.04.021

UAVs mission planning with flight level constraint using Fast Marching Square Method

V. González *, C.A. Monje, L. Moreno, C. Balaguer

System Engineering and Automation Department, University Carlos III of Madrid, Avenida Universidad 30, 28911 Leganés, Madrid, Spain

HIGHLIGHTS

- This study proposes a novel approach to solve the TFF problem at a certain altitude for different applications.
- The approach plans a feasible path for a UAV keeping a flight level with respect to the ground.
- The FM^2 algorithm is employed to plan a path avoiding any obstacles and keeping a flight level with respect to the ground.
- The smoothness and feasibility of the path are conditioned to parameters of the FM^2 algorithm.

ARTICLE INFO

Article history:
Received 21 February 2017
Received in revised form 25 April 2017
Accepted 30 April 2017

Keywords:
UAVs
Fast Marching Method
3D path planning
Mission planning
Flight level

ABSTRACT

In the last decade, Unmanned Aerial Vehicles (UAVs) have been a research focus for many purposes. Many of these studies require a path planning to perform autonomous flights, as well as the maintenance of a fixed flight level with respect to the ground to capture videos or overlying images. This article presents an approach to plan a mission for UAVs keeping a fixed flight level constraint. The 3D environment where the planning is carried out is an open field with non-uniform terrain. The approach proposed is based on the Fast Marching Square (FM^2) method, which generates a path free from obstacles. Our approach includes two adjustment parameters. Depending on the values of these parameters, the restriction of flight level can be modified, as well as the smoothness and safety of the generated paths. Simulated experiments carried out in this work demonstrate that the proposed approach generates trajectories respecting a fixed flight level over the ground with successful results.

1. Introduction

Unmanned Aerial Vehicles (UAVs) are a powerful tool to aid the human being in a wide range of applications of the twenty-first century. The demand of these aerial platforms, also known as drones, is given by several factors, among others: (1) tasks in dangerous conditions can be performed by them, without the necessity to be carried out by the human being [1]; (2) the cost of these aerial platforms is relatively low in comparison with other conventional platforms or satellites, and most of them have a high maneuverability.

These new tools, which can be autonomous and teleoperated, are used to manage different crisis presented in civil or military fields [2]. One of the areas nowadays where the research with UAVs is very extended is in post-disaster natural situations. The natural disasters affect millions of people each year. A quick management of the situation can reach to mitigate its consequences. Emergency communication systems [3], monitoring and mapping of disaster areas [4], design of humanitarian missions [5] and systems to assist search and rescue operation [6] are applications destined to reduce the number of victims and the economic impact. Another area where the use of UAVs is beneficial is the detection and tracking of high power lines [7]. The maintenance and detection of possible anomalies can avoid fires and putting the safety of the civilians at risk. Also, the road detection [8] and traffic monitoring [9] with UAVs are favorable to decrease the traffic congestion and the emissions. For a better crop management and monitoring, there are also applications where the UAVs provide a very flexible monitoring [10,11]. Each of these tasks needs to capture videos or a large number of overlapping images in order to achieve its purpose. The images must be captured with a high quality and with the same resolution.

It is clear that according to the specific application, the path planning requirements will be different. In the majority of the references given above, the applications translate into requirements concerning the following of a surface or tracking of certain objects in the environment, which implies to fix a certain flight level over

* Corresponding author.
E-mail addresses: vegonzal@ing.uc3m.es (V. González), cmonje@ing.uc3m.es (C.A. Monje), moreno@ing.uc3m.es (L. Moreno), balaguer@ing.uc3m.es (C. Balaguer).

the terrain or the objects to inspect. However, others like a nap-of-the-earth type of missions may impose other particular optimization requirements to be taken into account for the obtaining of the resulting path. For instance, in the previous work by the authors in [12], the path is planned at a constant height among the buildings of a city or above some of the buildings, according to the specific requirements of the mission.

The main objective in this work is to plan a mission to be carried out by a UAV in a 3D environment, keeping a flight level with respect to the ground, that is to say, a terrain following flight (TFF) at a certain altitude. In our case, the environment is an open field with mountainous terrain, whose obstacles are the mounds in the terrain.

Different techniques of path planning for UAVs have been studied in many works: Rapidly exploring random Tree (RRT) [13,14], A* and D* Search algorithms [15,16] or Probabilistic Roadmap Method (PRM) [17,18]; however, these works require many interactions and their paths often tend to be too long and need to be improved.

Besides, some of these path planning approaches do not consider flight restrictions, such as the terrain following at a fixed altitude. In the last decade, this problem has been studied in several works. For instance, [19,20] present methodologies for path planning and optimization in TFF, though the problem is treated only in 2D. A 3D terrain following/avoidance trajectory optimization is performed in [21], dividing the problem into two parts: first, the generation of the path, and second, a later optimization of the resulting path. In [22] the problem for Nap-of-the-earth is solved with a Mixed Integer Linear Programming (MILP). This method has a computational complexity given by $O(2^N)$, where N is the total number of sampling points. The main drawback of this function is that, as problem instances get very large, they will require large amounts of computing power to solve. A similar application is treated in [23], using optimal control theory. This type of control is characterized for being time-consuming, though the authors propose a novel approach to reduce the computational cost of the solution. These types of approaches have also been tested in real platforms [24].

In our case, the algorithm chosen as planner is the Fast Marching Square (FM^2). The low complexity of this method allows its use in different fields of planning, such as mobile vehicles [25,26] and vehicle formations in 2D [27] and 3D [28] environments, providing optimal trajectories in terms of smoothness and safety.

It should be taken into account that, when a path planning is carried out, the inclusion of certain constraints is of vital importance to obtain feasible paths. Most works where a planning is performed take into account restrictions within the UAV kinematic model [13,29,30]. To this respect, our approach has been proven to generate paths with adaptive smoothness and compatible with UAV kinematic restrictions, as demonstrated in [31], where the paths resulting from FM^2 are compared with those resulting from considering the Dubins Model.

As a further approach, and thanks to the introduction of two adjustment parameters, the algorithm will allow the path to fulfill both flight level and smoothness constraints so that it can be feasibly executed by a real UAV platform without the need to implicitly include its kinematic or dynamic model into the algorithm. This fact reduces considerably the computational cost of the approach, allowing it even to be executed in real time for dynamic environments. Besides, the approach provides a desired path just in one run, and no later optimization is required, unlike other works cited above, which also contributes to the reduction of the computational cost. In fact, the FM^2 is a planning method of order loglinear $O(N\log(N))$ [32], which, unlike the method used in [22] of exponential order, allows solving problems considerably greater in shorter time.

Fig. 1. The 3D simulated representation of the open field environment.

The contributions of this paper are as follows: (1) we introduce for the first time in the FM^2 method an approach in order to maintain a fixed flight level with respect to the ground; (2) the mission is optimized in terms of safety and smoothness running the approach only once. A future objective will be capturing videos and overlaying images of the terrain keeping an altitude, in order to perform surveillance and tracking tasks.

The advantages of our approach lie in the following aspects:

- Easy concept. The method is based on the natural movement of a wave, so conceptually, it is very easy to understand. Thanks to this, the imposition of the flight level constraint is simple to implement.
- Smoothed and safety trajectories. The method provides very smooth paths, since it is based on the propagation of a wave. Thus, the paths do not need to be refined in order to respect the kinematics of the UAV.
- Fast response. Though the expansion time of the wave depends on the complexity of the environment, the method has a fast and efficient computational speed.

The research of this article is organized as follows. Section 2 introduces the problem statement, the mission and the environment. A summary of the used path planning methods is presented in Section 3. The proposed approach to maintain a flight level with respect to the ground is presented in Section 4. Section 5 presents the simulation results from the application of the proposed approach. Finally, the conclusions and future works are presented in Section 6.

2. Problem statement

The problem statement is divided into two different issues: on the one hand, the environment where the mission is carried out is presented; and the other hand, the mission planning (goal) is described.

2.1. Environment

The environment where the mission planning is carried out is shown in Fig. 1. The represented environment is an open field with mountainous terrain where the surface is rather uneven, this being a 3D grid map with dimensions 120 × 90 × 40 cells. Each cell of the map is equivalent to 15 × 15 × 15 m. In this case, it is not necessary to consider the size of the UAV, since it is assumed to be smaller than the size of a cell. In the case that the UAV exceeds the size of the cell, the obstacles of the map can be swelled according to the radius of the vehicle, as demonstrated in [27].

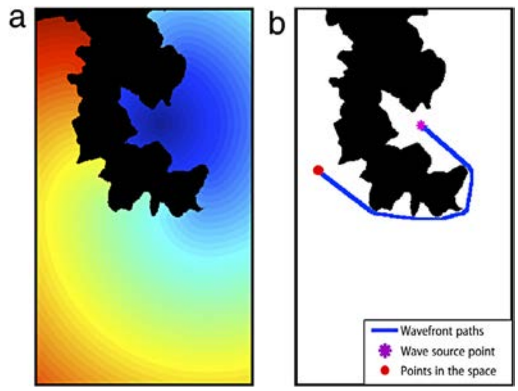

Fig. 2. Application of the FMM: (a) the time of arrival map; (b) the resulting path in the initial map.

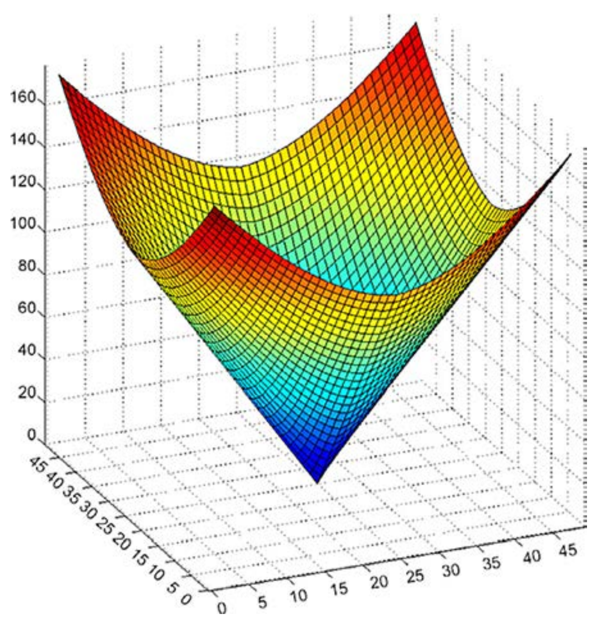

Fig. 3. The FMM applied in a 3D grid map.

2.2. Mission

Our mission requires a UAV moving throughout an open field environment, flying from a start position to a goal position, avoiding any hill in the terrain and maintaining a fixed flight level over the ground.

An approach based on the FM^2 method is used to find a path that joins two points with different configurations. This approach generates a path composed of a set of consecutive points such as $Q = P_0, P_1, \ldots, P_n$. To maintain a determined flight level with respect to the ground, two adjustment parameters are employed. The values of these parameters affect the compliance of the restriction in flight, depending on the desired smoothness and safety of the trajectory. This entire process is explained in Section 4.

3. Path planning methods

Nowadays, any autonomous vehicle application requires an optimal path planning. The generated trajectories must be safe and smooth in order to be followed faithfully by the vehicle. The method chosen here as planner is the FM^2 method, which is based on applying the Fast Marching Method (FMM) twice. The FMM explains how a wave is expanded in a media, as if it was a thick liquid. A summary of these two methods is presented next.

3.1. Fast Marching Method

The FMM is a numerical algorithm that solves the arrival time of an expanding wave in every point of the space. The FMM was introduced by Sethian in 1996 [33] and is a particular case of level set methods [34] where the wave is always expanded forward, that is to say, with non-negative velocity.

The fundamental base of the FMM is the same as the Fermat principle in optics, which established in short, that the light traveling between two points always chooses the optimal path in terms of time.

The wave propagation is described by the Eikonal equation, where $\boldsymbol{\rho}$ is a point of the space, $T(\boldsymbol{\rho})$ is the arrival time of the wave front and $F(\boldsymbol{\rho})$ is the propagation speed of the wave:

$$1 = F(\rho)|\nabla T(\rho)|. \tag{1}$$

The point where the wave is born is ρ_0, its time being $T_0 = 0$. When the wave starts expanding, the FMM computes in each iteration the time $T_{i,j}$ for each point of the space $x_{i,j}$, according to the discretization of the Eikonal equation:

$$\max\left(\frac{T - T_1}{\triangle x}, 0\right)^2 + \max\left(\frac{T - T_2}{\triangle y}, 0\right)^2 = \frac{1}{F_{i,j}^2}, \tag{2}$$

where $F_{i,j}$ is the expansion speed of the wave for each point of the grid, $\triangle x$ and $\triangle y$ are the grid spacing for the directions of x and y, respectively, and

$$\begin{aligned} &T = T_{i,j}, \\ &T_1 = \min(T_{i-1,j}, T_{i+1,j}), \\ &T_2 = \min(T_{i,j-1}, T_{i,j+1}). \end{aligned} \tag{3}$$

This process is meticulously explained in [35]. The result is the distance map shown in Fig. 2(a), also denoted as time of arrival map. In order to obtain the trajectory shown in Fig. 2(b), the gradient descent is applied in any point of the time of arrival map up to the source point of the wave.

Although the FMM has been explained for a bidimensional map, it can be used for n dimensions. If the FMM is applied in a 3D environment the result is shown in Fig. 3 [36], where it is appreciated that the wave is expanded until the highest point of the z axis ($F > 0$), with a single global minima.

It should be noted that the FMM generates optimal trajectories in terms of time, but its curves suffer abrupt changes and are very close to the obstacles (see Fig. 2(b)). This is due to the fact that the geodesic loses their smoothness when abrupt changes are produced in the velocity wave [26]. The FM^2 method solves these problems, as explained next.

3.2. Fast Marching Square Method

The FM^2 was introduced by Garrido et al. in 2009 [37] and consists on applying the FMM twice. This method solves the problem mentioned in the previous section, providing paths with an adequate smoothness and sufficient safety distances from the obstacles. The following procedure describes how the FM^2 method works:

1. The 3D environment used as an input, W_0, is read as a binary grid map (see Fig. 4(a)). The cells belonging to obstacles are labeled in black (value 0) and the cells of free space are labeled in white (value 1).

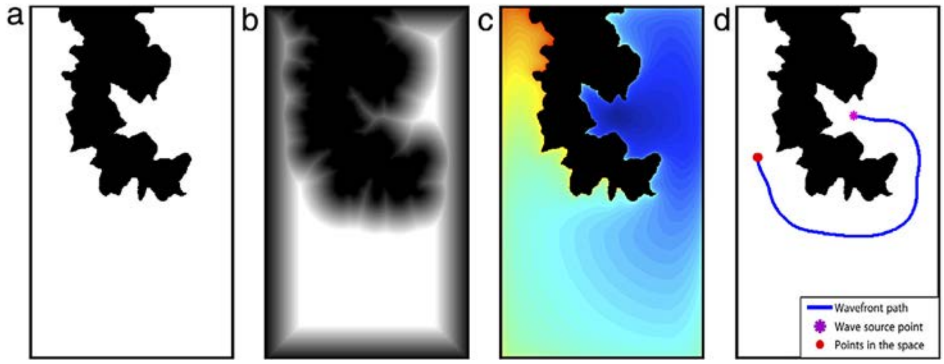

Fig. 4. Application of the FM^2 method: (a) map read as binary gridmap; (b) the Velocities map F; (c) the time of arrival map T; (d) the resulting path in the initial map.

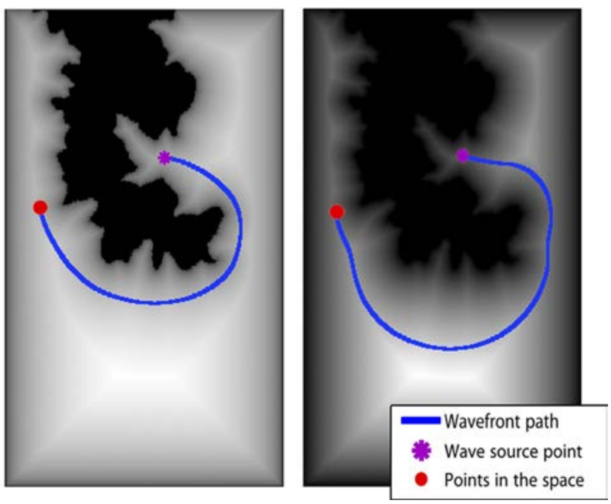

Fig. 5. The map F raised to different values and their respective paths.

2. The FMM is applied over the binary map (Fig. 4(a)) using each cell belonging to the obstacles as wave source, expanding several waves at the same time. In this way, each cell of the map acquires a certain value, which is the time that the wave takes to reach each point of the space. The resulting map is rescaled to fix the maximum cell value as 1. Then, each cell has a value between 0 and 1. The resulting map is a potential field of the original map denominated velocities map (F), as shown in Fig. 4(b). This map is denoted so because the value of each cell is proportional to the distance from obstacles and it can be interpreted as the velocity of the vehicle at the same time. So, F provides the maximum admissible speed at each point of the environment. That is to say, if the vehicle is near the obstacles, the admissible speed will be less than if the vehicle is away from the obstacles.
3. The FMM is applied again from the goal point, using this point as wave source. The wave is expanded over the map F until the start point is reached. Fig. 4(c) shows the time of arrival map T as the result of this process.
4. The gradient descent is applied over T from the start point to the goal point obtaining the optimal path in terms of smoothness and safety, as shown in Fig. 4(d).

Although the paths generated by the FM^2 are good in terms of safety and smoothness, those paths are often not sufficiently optimal for the proposed mission. Therefore, the planning can be modified by an adjustment parameter according to the requirements of the mission planning.

Each cell of the map F is raised to this adjustment parameter, increasing or decreasing its value. This causes a lightening or darkening of each cell in accordance with the value of that parameter. The greater the adjustment parameter, the greater the darkening of the map F, causing paths further away from the obstacles. On the contrary, if the value is lower, the map F is clarified and this will generate smoother paths closer to the obstacles. This process is illustrated in Fig. 5.

The map F is saturated according to the different constraints that should be taken into account when the planning is carried out. In our case, F is saturated to obtain certain security margins and smoothness in the path. So, the speed is also modified due to this saturation. If the map is obscured the permissible speed of the vehicle will be lower than if the map is clarified. According to this, the speed of the UAV is a consequence of the treatment of the map.

In our approach, two adjustment parameters p_1 and p_2 are used: one of them is used to clarify the map cells where the path has to be planned, and the other is used to obscure the rest of the map cells.

The map F can be modified to attend to other optimization criteria, as demonstrated in [25] and [38] by some of the authors of this work. One of the cost functions to be implemented could be related to fuel optimization, for instance.

In this approach, however, the map F is changed by parameters p_1 and p_2 to optimize the smoothness of the trajectory in order to meet the UAV kinematic constraints. The smoothness is characterized by the turn angle, climb angle and curvature profiles of the path. Though these profiles affect directly the performance of the UAV with respect, for instance, to its fuel cost, a deeper characterization of these relationships is out of the topic of this paper and has not been considered.

4. Path planning with flight level constraint

This section presents our approach to carry out the path planning in a 3D open field environment where a flight level is imposed over the ground. This flight level must be respected by the UAV in the trajectory, considering that the initial and final stretches do not respect this constraint due to the configuration of the start and final points of the trajectory.

The chosen environment to perform the planning is described in Section 2 and the planner is the FM^2 method. An approach to plan trajectories with an imposed flight level over the ground is added within the FM^2 method.

As stated in Section 3, the wave front used in the FM^2 method tends to expand by the clearer areas of the map F. Therefore, the value of the cells where we want to 'force' the planning must be close to 1. It is noteworthy that the environment map is a 3D grid map, so the different layers of the map F can be clarified or obscured as shown in Fig. 6.

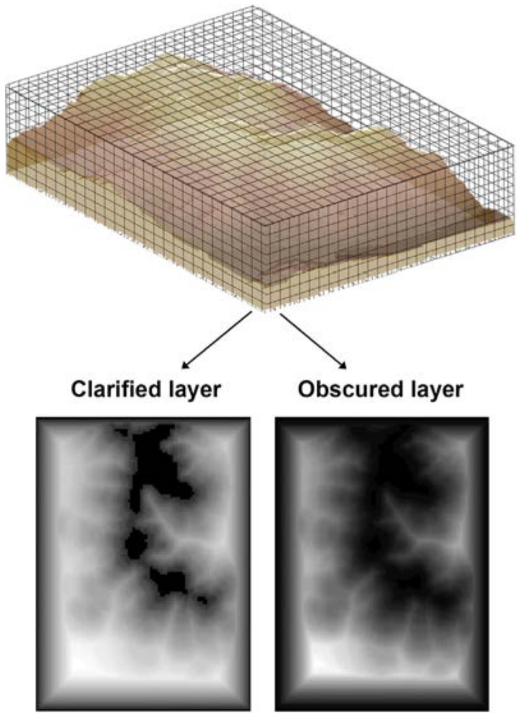

Fig. 6. The upper part of the image shows the 3D grid map of the environment. The lower part shows clarified and obscured layers of the map F.

To achieve our goal, the corresponding cells with the fixed flight level over the ground have to be clarified. Algorithm 1 presents the approach used within the FM^2 to fix a flight level with respect to the ground. For this purpose, two adjustment parameters, p_1 and p_2, are employed. The mission of each of these parameters is to clarify or darken the map F cells according to the desired planning.

Algorithm 1 Imposition of a fixed flight level with respect to the ground.

Require: The Velocities map F of a gridmap G of size m x n x l.
Require: Flight level L_f with respect to the ground.
Require: Adjustment parameters p_1 and p_2.
Ensure: The Velocities map F with the clarified flight level cells.

1: **for** k **to** l **do**
2:   **for** j **to** n **do**
3:     **for** i **to** m **do**
4:       $SurfaceValue \leftarrow Surface(i, j)$
5:       **if** $k = (L_f + SurfaceValue)$ **then**
6:         $f_{i,j,k} \leftarrow (f_{i,j,k})^{p_1}$
7:       **else**
8:         $f_{i,j,k} \leftarrow (f_{i,j,k})^{p_2}$
9:       **end if**
10:     **end for**
11:   **end for**
12: **end for**

The procedure to modify the value of the map F cells belonging to the given flight level over the ground is as follows:

- Firstly, the terrain elevation for each cell of the map, $Surface(i, j)$, is identified (see Algorithm 1, line 4). This elevation is computed taking as reference the layer 0 of the environment, which can be defined as sea level.
- Then, the value of the given flight level is added to the value of the terrain elevation (Algorithm 1, line 5). These cells are clarified raising its value to p_1 (Algorithm 1, line 6). Thus, the planning for these zones will be easier.
- The rest of the cells are obscured raising them to p_2 (Algorithm 1, line 8), making the planning harder through them.

The influence of the values of parameters p_1 and p_2 on the smoothness and feasibility of the path will be discussed in detail in next section.

Though this work does not deal with the uncertainty problem, our approach can be used in case of terrain uncertainties or even dynamic obstacles avoidance. A previous work by the authors [27] focuses on this topic.

In the case of terrain uncertainties, the procedure will depend on their characteristics. For instance, if there is a total uncertainty on a particular part of the map and that region model is not known, then one extreme alternative could be not to include that region in the planning in order to avoid passing through it. On the contrary, if the terrain uncertainties can be quantified and the uncertainty range is well defined, then that range can be included in the planning as a security margin, enlarging the corresponding areas in the map so that the algorithm treats them as enlarged obstacles.

When the uncertainties are somehow limited but cannot be defined with precision, then the algorithm can be locally executed during the flight around those regions with uncertainties, with a specific time interval between executions, depending on the rate of change of the environment [27]. For this, the UAV must be equipped with the corresponding sensors to detect and measure the uncertainty in real time. A more detailed study of the treatment of this type of terrain uncertainty will be addressed in future works by the authors.

5. Simulation results

The approach described in the previous section has been run under the toolbox Fast Marching provided by Peyre [39] using Matlab 2013a and the code for N-dimension given in [40]. The computer used is a standard one with operating system Ubuntu 14.04. Algorithm 1 proposed in Section 4 for the imposition of the flight level and adjustment of the path smoothness has been programmed in Matlab in the context of the previously cited codes and run for the 3D environment described in Section 2. The results obtained from this approach are presented next.

Having taken the start and goal points of the trajectory, the approach based on the FM^2 method takes the simulated environment and plans the trajectory with a fixed flight level with respect to the ground, avoiding any hill above the terrain.

Two experiments have been carried out, where the adjustment parameters p_1 and p_2 are used to modify the map F and thus to impose a constraint over the flight level maintained by the UAV. The first experiment analyzes how the planning maintains a fixed flight level with respect to the ground. In the second experiment, the trajectory smoothness is studied according to the difference between the values of p_1 and p_2. In this latter experiment it is shown how the smoothness of the trajectory can affect the compliance of the flight level constraint, since the terrain is highly non-uniform.

5.1. Different flight levels with respect to the ground

The aim of this experiment is to plan the optimal trajectories respecting a given fixed flight level with respect to the ground. Three different cases are presented in this experiment: the first case is evaluated with a flight level of 2 over the ground; the second one with a flight level of 5; and the third one with a flight level of 10. The start and goal points are the same in all the cases, being $p_s(20, 20, 20)$ and $p_g(100, 80, 30)$, respectively.

To maintain a fixed flight level with respect to the ground, it is necessary to adjust the values of p_1 and p_2, which affect the map F.

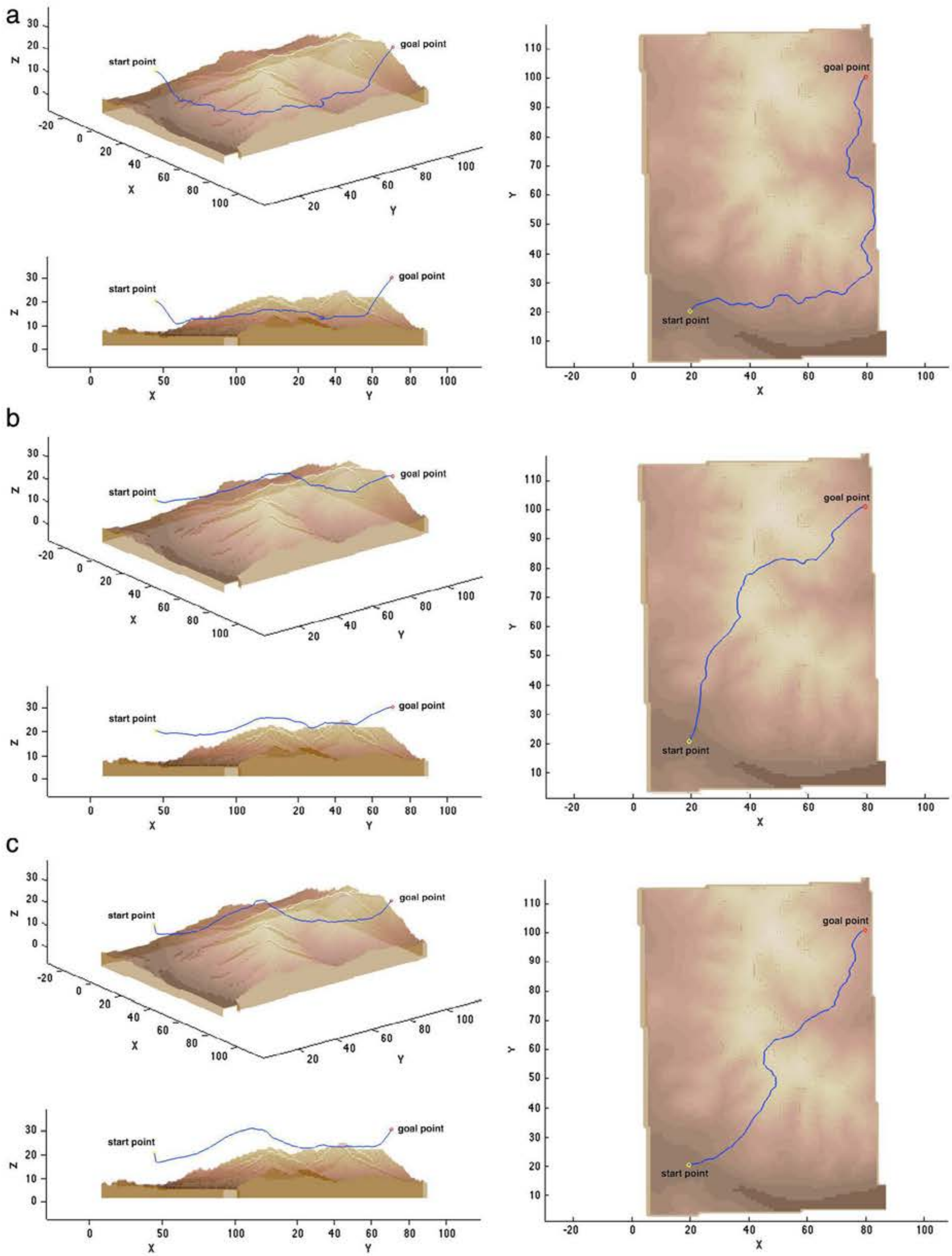

Fig. 7. Paths at different flight levels with respect to the ground: (a) path at flight level 2; (b) path at flight level 5; (c) path at flight level 10.

5.1.1. Case 1

For the first case, the values of p_1 and p_2 are adjusted to 0.5 and 2.5, respectively, for a flight level of 2. The result is shown in Fig. 7(a). The planned path avoids the central mountain and is planned by the lateral areas of the map, where the terrain is more uniform. That is because the value of p_2 is very high. This produces a much greater darkening of the upper layers, causing a planning less permissive.

Fig. 8(a) shows the representation of the simulated path (resulting path from FM^2) with respect to the ideal path and the terrain in the plane *yz* for a flight level of 2. As can be appreciated, the difference between the simulated path and the ideal path is

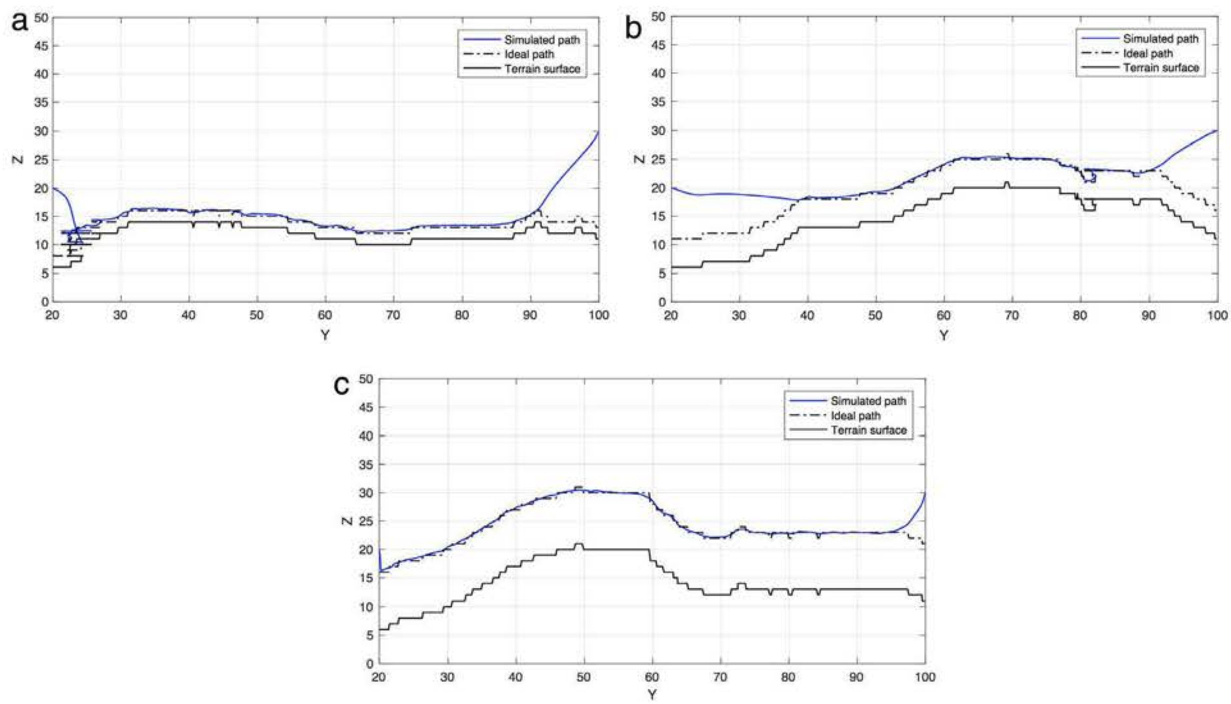

Fig. 8. Comparison of the resulting path against the ideal path and the profile terrain: (a) path at flight level 2; (b) path at flight level 5; (c) path at flight level 10.

minimal. The only exceptions are the initial descent and the final ascent due to the position of the start and goal points, respectively, whose slopes are imposed by the smoothness of the planning.

5.1.2. Case 2

In the second case, p_1 and p_2 are adjusted to 0.5 and 1.5, respectively, in order to maintain a flight level of 5. Fig. 7(b) shows the results. In this case, the path is planned along the center of the map, since the value of p_2 is smaller than in the previous case and the planning is more permissive, allowing to plan the path through the upper layers.

Fig. 8(b) shows the simulated path with respect to the ideal path and the terrain in the plane *yz* for a flight level of 5. The simulated path tries to follow the terrain. Like in the previous case, the difference between the simulated path and the ideal path are minimal with the exception of the stretches belonging to the descent and ascent of the trajectory at the start and goal points.

5.1.3. Case 3

The last case of this experiment is shown in Fig. 7(c), where $p_1 = 0.5$ and $p_2 = 1.3$ in order to maintain a flight level of 10. As in the previous case, the trajectory is also planned through the center of the map.

Fig. 8(c) shows the simulated path with respect to the ideal path and the terrain in the plane *yz* for a flight level of 10. The altitude variation is smaller than in the previous cases, even at the initial and final stretches of the path, since the smoothness of the trajectory is more compatible with the planning requirements.

As a conclusion, it can be seen that in all cases the flight level is respected with small variations, depending of the smoothness imposed by the planning.

5.2. Different smoothness of the trajectory

This second experiment analyzes how the trajectory can be smoothed according to the difference between the values of parameters p_1 and p_2. Here, two cases are studied where the variation of the trajectory is appreciated when modifying the values of the adjustment parameters. The start and goal points are the same as in the first experiment and the trajectory is planned at a flight level of 10.

5.2.1. Case 1

For this first case, the value of p_1 has been maintained to 0.5 and the value of p_2 has been reduced to 1.0. The result is shown in Fig. 9(a). If this figure is compared with Fig. 7(c), it can clearly be seen that the planning is smoother. The planning is carried out through zones where the terrain is less pronounced. Furthermore, the curves and the ascents and descents are also less sharp.

5.2.2. Case 2

In the second case of this experiment, the difference between the values of the adjustment parameters has been decreased, being $p_1 = 0.5$ and $p_2 = 0.8$. In this case, the trajectory is much smoother than in the previous cases, as can be seen in Fig. 9(b). The curves and the altitude changes are less sharp.

Fig. 10 shows the simulated path against the ideal path and the terrain for a flight level of 10 for both experiments. The resulting paths travel through different areas of the map, and the turn angle, climb angle and curvature of the trajectories also vary, as demonstrated in Fig. 11, Fig. 12 and Fig. 13, respectively. As can be appreciated, the turn angle, climb angle and curvature profiles of the path in Case 1 are more pronounced than those in Case 2. These profiles are related to the smoothness of the path and therefore can be adjusted by parameters p_1 and p_2.

From the set of experiments carried out in this section, it can be concluded that the smoothness and feasibility of the path are conditioned to parameters p_1 and p_2. Apart from their absolute values, the relationship between them (difference of their values) has an important role. If that difference is small, the trajectory will be more optimal in terms of smoothness and safety. On the contrary, if the difference is bigger, the generated trajectory will have sudden changes of altitude and sharper curves, but will faithfully follow the profile of the terrain.

This can be used as a first design criterion when setting the initial values of these parameters in order to adapt the smoothness

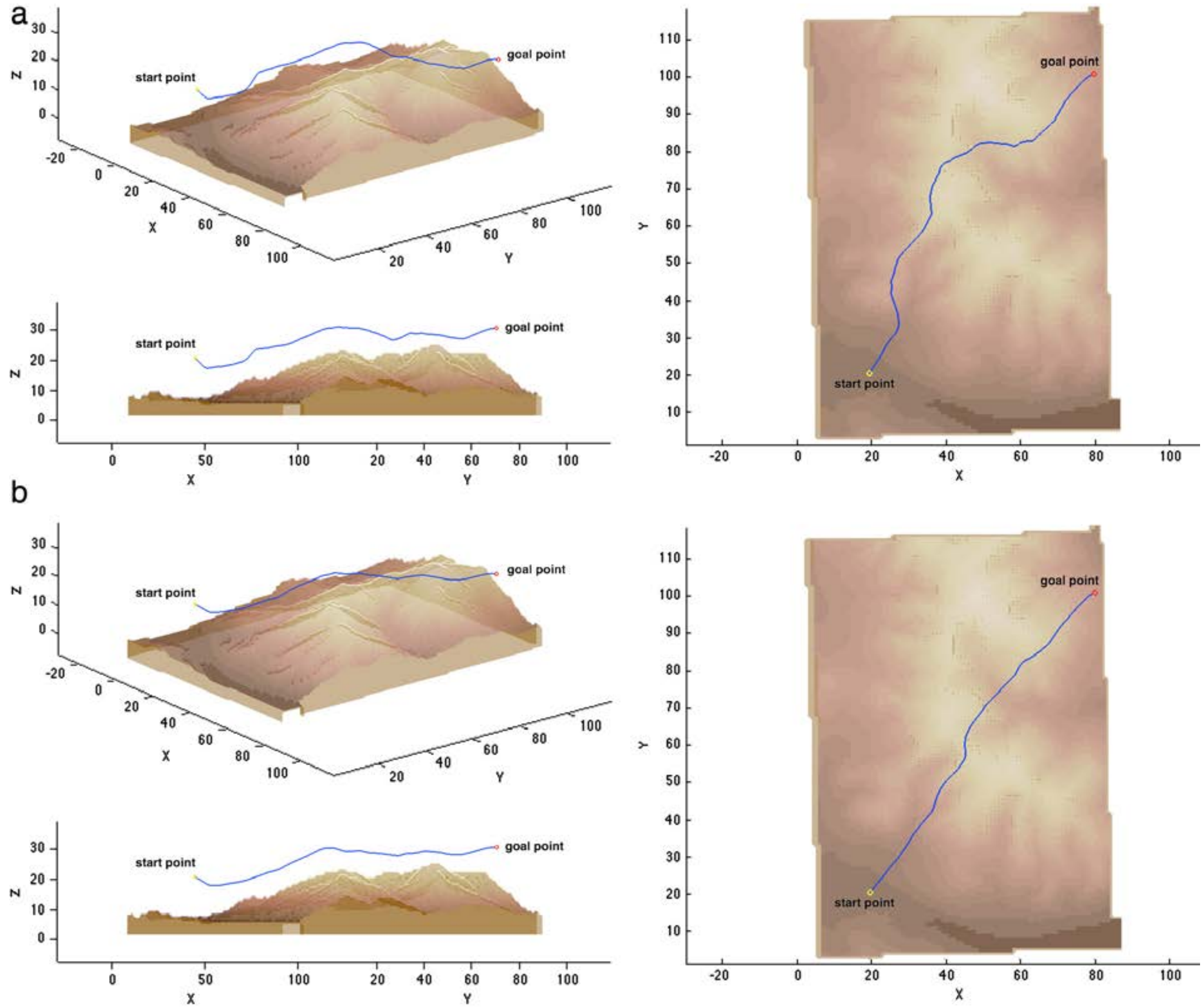

Fig. 9. Paths at flight level 10 with different smoothness: (a) $p_1 = 0.5$ and $p_2 = 1$; (b) $p_1 = 0.5$ and $p_2 = 0.8$.

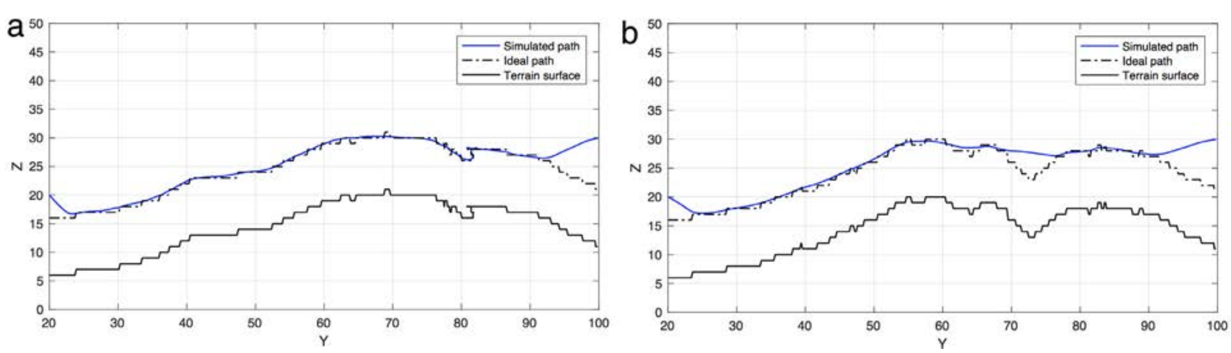

Fig. 10. Comparison of the resulting path against the ideal path and the terrain profile: (a) $p_1 = 0.5$ and $p_2 = 1$; (b) $p_1 = 0.5$ and $p_2 = 0.8$.

of the path and make it more feasible for its execution by the UAV from the very beginning. In case the kinematic constraints of turn angle, climb rate or curvature are not fulfilled at a first run, or on the contrary, allow the obtaining of a more refined path over the terrain, the parameters can be changed according to these design rules in order to meet the requirements.

It is clear that the optimality problem in this case depends very much on restrictions for the algorithm coming from optimization constraints such as the kinematics of the UAV or its dynamics, as discussed in the paper. And even more, other constraints such as fuel consumption could be considered and will affect the optimal $p_1 - p_2$ sets of values. We are somehow dealing with a Pareto optimality problem that needs an accurate definition of the optimization criteria.

A further research step is currently focusing on the study of the explicit relationship between the UAV kinematics and the value of the adjustment parameters, as a first approach to the optimality study.

With our approach so far, it is expected that a feasible path can be obtained at a first run, as demonstrated in [31], where the paths

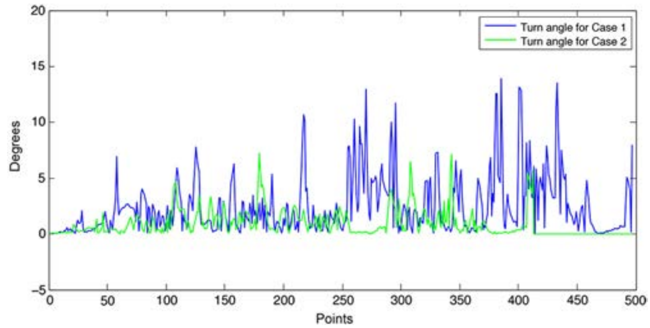

Fig. 11. Profile of the turn angle for different smoothness of the trajectory.

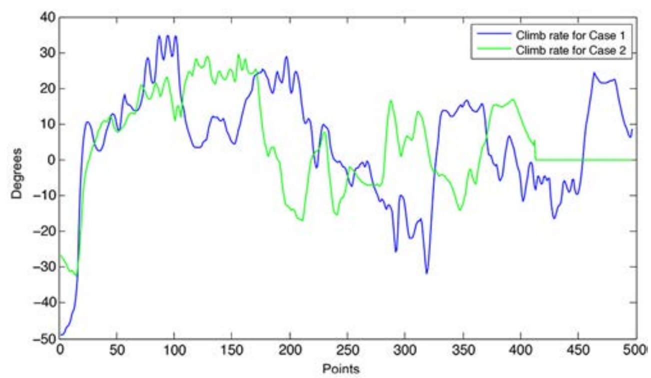

Fig. 12. Profile of the climb angle for different smoothness of the trajectory.

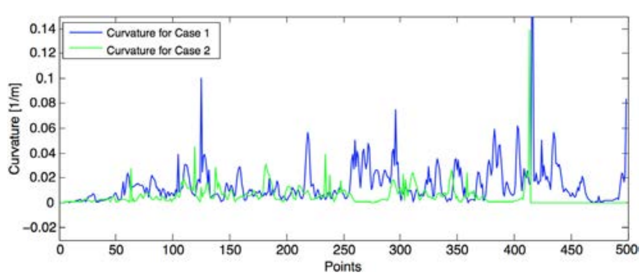

Fig. 13. Profile of the curvature for different smoothness of the trajectory.

resulting from FM^2 are compared with those from considering the Dubins kinematic model of a UAV. In any case, the turn angle, climb angle and curvature curves in Fig. 11, Fig. 12 and Fig. 13, respectively, can be obtained and used to check the feasibility of the paths for every specific 3D environment and particular kinematic restrictions.

Besides, from the profiles in Figs. 11–13, and after several mathematical computations, the dynamic restrictions for the UAV with respect to speed and acceleration ranges can be determined. This dynamic study will be done in a future work in order to reach an analytical and explicit relation between parameters p_1 and p_2 and the permissible dynamic ranges of the UAV.

In order to simplify the study on the relationship between the kinematic and dynamic restrictions and the values of the adjustment parameters, these two can be established by fixing $p_1 = 1$ and varying p_2, or setting $p_1 = k$ and $p_2 = 1 - k$ and then setting k to different values to create different paths. The introduction of parameter k to rule that relationship can help to simplify future studies.

6. Conclusions and future works

This work presents a novel approach based on the FM^2 method to plan a trajectory for a UAV maintaining a given flight level with respect to the ground. This planning has been carried out in an open field environment with non-uniform terrain. The method generates the optimal trajectory in terms of smoothness and safety from a start point to a final point, avoiding any mound (obstacle) on the terrain.

Two adjustment parameters p_1 and p_2 have been used to force the path planning in specified areas of the 3D map determined by a given flight level. As a result, the modification of p_1 and p_2 causes variations in the cells of the Velocities map F, producing its lightening or darkening. To maintain an altitude over the ground, the gridmap cells whose value is the sum of the terrain elevation plus the flight level are clarified, while the rest of the cells are obscured. Consequently, the path planning is performed through the clearer zones, where the wave front of FM^2 has much more facility to expand, thus maintaining the specified flight level.

The results have also shown that the modification of the path in terms of smoothness and safety is caused by the variation of the difference between the values of the adjustment parameters. Besides, the greater the smoothness, the lower the probability that the path faithfully follows the profile of the terrain.

In a further research, the explicit relationship between the adjustment parameters and the kinematic and dynamic constraints of the UAV will be analyzed, as a first approach to the optimality study.

Acknowledgment

The research leading to these results has received funding from the RoboCity2030-III-CM project (Robótica aplicada a la mejora de la calidad de vida de los ciudadanos, fase III; S2013/MIT-2748), funded by Programas de Actividades I+D en la Comunidad de Madrid and cofunded by Structural Funds of the EU.

References

[1] C.A.F. Ezequiel, M. Cua, N.C. Libatique, G.L. Tangonan, R. Alampay, R.T. Labuguen, C.M. Favila, J.L.E. Honrado, V. Caños, C. Devaney, A.B. Loreto, J. Bacusmo, B. Palma, UAV aerial imaging applications for post-disaster assessment, environmental management and infrastructure development, in: Proc. Int. Conf. Unmanned Aircr. Syst., ICUAS, 2014, pp. 274–283.

[2] L. Zhong, Q. Luo, D. Wen, S.D. Qiao, A task assignment algorithm for multiple aerial vehicles to attack targets with dynamic values, IEEE Trans. Intell. Transp. Syst. 14 (1) (2013) 236–248.

[3] G. Tuna, B. Nefzi, G. Conte, Unmanned aerial vehicle-aided communications system for disaster recovery, J. Netw. Comput. Appl. 41 (2014) 27–36.

[4] G. Nugroho, Z. Taha, T.S. Nugraha, H. Hadsanggeni, Development of a fixed wing unmanned aerial vehicle (UAV) for disaster area monitoring and mapping, J. Mechatron. Electr. Power Veh. Technol. 6 (2015) 83–88.

[5] T. Tanzi, L. Apvrille, J.-L. Dugelay, Y. Roudier, UAVs for humanitarian missions: Autonomy and reliability, in: Proc. IEEE 2014 Glob. Humanit. Technol. Conf., 2014, pp. 271–278.

[6] Y.-H. Ho, Y.-R. Chen, L.-J. Chen, Krypto: Assisting search and rescue operations using Wi-Fi signal with UAV, in: Proc. First Workshop on Micro Aer. Veh. Netw. Syst. Appl. Civ. Use, Florence, Italy, 2015, pp. 3–8.

[7] C. Martinez, C. Sampedro, A. Chauhan, P. Campoy, Towards autonomous detection and tracking of electric towers for aerial power line inspection, in: 2014 Int. Conf. Unmanned Aircr. Syst., ICUAS, 2014, pp. 284–295. http://dx.doi.org/10.1109/ICUAS.2014.6842267.

[8] H. Zhou, H. Kong, L. Wei, D. Creighton, S. Nahavandi, Efficient road detection and tracking for unmanned aerial vehicle, IEEE Trans. Intell. Transp. Syst. 16 (1) (2015) 297–309.

[9] K. Kanistras, G. Martins, M.J. Rutherford, K.P. Valavanis, A survey of unmanned aerial vehicles (UAVs) for traffic monitoring, in: 2013 Int. Conf. Unmanned Aircr. Syst., ICUAS, 2013, pp. 221–234. http://dx.doi.org/10.1109/ICUAS.2013.6564694.

[10] J. Primicerio, S.F.D. Gennaro, A.L.G. Edoardo Fiorillo, E. Lugato, A. Matese, F.P. Vaccari, A flexible unmanned aerial vehicle for precision agriculture, J. Precis. Agric. 13 (4) (2012) 517–523.

[11] D. Gómez-Candón, A.I.D. Castro, F. López-Granados, Assessing the accuracy of mosaics from unmanned aerial vehicle (UAV) imagery for precision agriculture purposes in wheat, J. Precis. Agric. 15 (2014) 44–56. http://dx.doi.org/10.1007/s11119-013-9335-4.
[12] V. González, C.A. Monje, L. Moreno, C. Balaguer, UAVs mission planning with imposition of flight level through fast marching square, J. Cybern. Syst. (2017) 1–12. http://dx.doi.org/10.1080/01969722.2016.1263521.
[13] Y. Lin, S. Saripalli, Path planning using 3D dubins curve for unmanned aerial vehicles, in: Int. Conf. Unmanned Aircr. Syst., 2014, pp. 296–304.
[14] A.J. Ten-Harmsel, I.J. Olson, E.M. Atkins, Emergency flight planning for an energy-constrained multicopter, J. Intell. Robot. Syst. 85 (2017) 145–165.
[15] B. Zhang, L. Tang, M. Roemer, Probabilistic weather forecasting analysis for unmanned aerial vehicle path planning, J. Guid. Control Dyn. 37 (1) (2014) 309–312.
[16] Q. Xue, P. Cheng, N. Cheng, Offline path planning and online replanning of UAVs in complex terrain*, in: Proc. 2014 IEEE Chinese Guid. Navig. Control Conf., 2014, pp. 2287–2292.
[17] F. Yan, Y. Liu, J. Xiao, Path planning in complex 3D environments using a probabilistic roadmap method, Int. J. Autom. Comput. 10 (6) (2014) 525-533.
[18] K. Obermeyer, P. Oberlin, S. Darbha, Sampling-based path planning for a visual reconnaissance unmanned air vehicle, J. Guid. Control Dyn. 35 (2) (2012) 619–631.
[19] S.M. Malaek, A.R. Kosari, Novel minimum time trajectory planning in terrain following flights, IEEE Trans. Aerosp. Electron. Syst. 43 (1) (2007) 2–12.
[20] K. Amirreza, M. Hossein, F. Mehdi, A new method for trajectory optimization in terrain following flight, in: 22nd Iran. Conf. Electr. Eng., ICEE 2014, 2014, pp. 1203–1208.
[21] R. Kamyar, E. Taheri, Aircraft optimal terrain/threat-based trajectory planning and control, J. Guid. Control Dyn. 37 (2) (2014) 466–483.
[22] C.S. Ma, R.H. Miller, Mixed integer linear programming trajectory generation for autonomous nap-of-the-earth flight in a threat environment, in: Proc. IEEE Aerosp. Conf., 2005, pp. 1–9.
[23] P.K.A. Menon, E. Kim, Optimal trajectory synthesis for terrain-following flight, J. Guid. Control Dyn. 14 (4) (1991) 807–813.
[24] B. Herisse, T. Hamel, R. Mahony, F.-X. Russotto, A terrain-following control approach for a VTOL Unmanned Aerial Vehicle using average optical flow, Auton. Robot. 29 (3) (2010) 381–399.
[25] S. Garrido, M. Malfaz, D. Blanco, Application of the fast marching method for outdoor motion planning in robotics, J. Robot. Auton. Syst. 61 (2) (2013) 106–114.
[26] J. Gómez, A. Vale, S. Garrido, L. Moreno, Performance analysis of fast marching-based motion planning for autonomous mobile robots in ITER scenarios, J. Robot. Auton. Syst. 63 (2015) 36–49.
[27] J. Gómez, A. Lumbier, S. Garrido, L. Moreno, Planning robot formations with fast marching square including uncertainty conditions, J. Robot. Auton. Syst. 61 (2) (2013) 137–152.
[28] D. Alvarez, J. Gómez, S. Garrido, L. Moreno, 3D robot formations planning with fast marching square, in: Proc. IEEE Int. Conf. Auton. Robot Syst. and Compet., 2014, pp. 59–64.
[29] O.K. Sahingoz, Generation of bezier curve-based flyable trajectories formulti-UAV systems with parallelgenetic algorithm, J. Intell. Robot. Syst. 74 (2014) 499–511.
[30] Z. Xing, C. Jie, X. Bin, P. Zhihong, A memetic algorithm for path planning of curvature-constrained UAVs performing surveillance of multiple ground targets, Chin. J. Aeronaut. 27 (3) (2014) 622–633.
[31] V. González, C.A. Monje, L. Moreno, C. Balaguer, Fast marching square method for UAVs mission planning with consideration of Dubins model constraints, in: Proc. 20th IFAC Symp. Autom. Control in Aerosp. (ACA), vol. 49, Sherbrooke, Quebec, Canada, 2016, pp. 164–169.
[32] G. Peyré, M. Péchaud, R. Keriven, L.D. Cohen, Geodesic methods in computer vision and graphics, Found. Trends Comput. Graph. Vis. 5 (3–4) (2010) 197–397.
[33] J. Sethian, A fast marching level set method for monotonically advancing fronts, Proc. Natl. Acad. Sci. USA 93 (4) (1996) 1591-1595.
[34] S. Osher, J. Sethian, Fronts propagating with curvature-dependent speed algorithms based on Hamilton–Jacobi formulations, J. Comput. Phys. 79 (1) (1988) 12–49.
[35] J.V. Gómez, Fast Marching Methods in Path and Motion Planning: Improvements and High-Level Applications, (Ph.D. thesis), Dept. Syst. Eng. Autom., Univ. Carlos III, Madrid, Spain, 2015.
[36] A. Valero-Gomez, J.V. Gómez, S. Garrido, L. Moreno, Fast marching methods in path planning, IEEE Robot. Autom. Mag. 20 (4) (2013) 111–120.
[37] S. Garrido, L. Moreno, M. Abderrahim, D. Blanco, FM2: a real-time sensor-based feedback controller for mobile robots, Int. J. Robot. Autom. 24 (1) (2009) 3169–3192.
[38] S. Garrido, L. Moreno, D. Alvarez, Path planning for mars rovers using the fast marching method, in: Robot 2015: Second Iber. Robot. Conf., vol. 1, Springer International Publishing, 2015, pp. 93–105. http://dx.doi.org/10.1007/978-3-319-27146-0_8.
[39] G. Peyre, Toolbox Fast Marching, 2004. URL goo.gl/cor8cs. (Accessed 17 February 2017).
[40] J.V. Gómez, J. Pardeiro, P. Gely, N-Dimensional Fast Marching Method V1.0, 2015. URL goo.gl/iaBFn3 (Accessed 15 February 2017).

Verónica González received the B.Sc. Industrial Engineering specialized in Electronics from the University of Castilla-La Mancha, Toledo, Spain in 2011. In 2013 she got a Master's degree in Robotics and joined the Department of Systems Engineering and Automation, University Carlos III of Madrid (UC3M). Currently, she is a Ph.D. student in the same department, at Robotics Lab. As a researcher focused in path planning for unmanned aerial vehicles.

Concepción A. Monje received her M.Sc. Degree in Electronics Engineering from the Industrial Engineering School of the University of Extremadura, Spain, in 2001, and her Ph.D. Degree in Industrial Engineering from the University of Extremadura, Spain, in 2006. In September 2006 she joined the University Carlos III of Madrid as a Visiting Professor in the Department of Systems Engineering and Automation. Her research focuses on control theory and applications of fractional calculus in control systems and robotics. She has been working in these areas for over 10 years, and she has published over 50 technical papers mostly related to control and robotics.

Luis Moreno received the B.Sc. degree in Automation and Electronics Engineering and the Ph.D. degree from the Polytechnic University of Madrid (UPM), Spain, in 1984 and 1988, respectively. From 1988 to 1994, he was an Associate Professor with the Polytechnic University of Madrid. In 1994, he joined the Department of Systems Engineering and Automation, UC3M, where he has been involved in several mobile robotics projects. His research interests include mobile robotics, mobile manipulators, environment modeling, path planning, and mobile robot global localization problems.

Carlos Balaguer received his Ph.D. in Automation from the Polytechnic University of Madrid (UPM), Spain, in 1983. From 1983–1994 he was with the Department of Systems Engineering and Automation of the UPM as Associated Professor. Since 1996, he has been a Full Professor of the Robotics Lab at the University Carlos III of Madrid. He is currently the Vice-chancellor for research of the University. His research has included humanoid and assistive and service robots, among others. He participates in numerous EU projects since 1989, such as Eureka projects SAMCA, AMR and GEO, Esprit projects ROCCO and CEROS, Brite project FutureHome, IST project MATS, and the 6FP IP projects ManuBuild, I3CON, and Strep Robot@CWE. He has published more than 180 papers in journals and conference proceedings, and several books in the eld of robotics.